European Biophysics Journal (2023) 52:131–143
https://doi.org/10.1007/s00249-023-01651-2

ORIGINAL ARTICLE

Revealing the single-channel characteristics of OprD (OccAB1) porins from hospital strains of *Acinetobacter baumannii*

Aliakbar Ebrahimi[1,4] · Tuğçe Ergün[1,7] · Özge Kaygusuz İzgördü[2] · Cihan Darcan[3] · Hüseyin Avci[4,8,9,10] · Barçin Öztürk[5] · Hatice Rahmet Güner[6] · Hamed Ghorbanpoor[4,11] · Fatma Doğan Güzel[1]

Received: 7 June 2022 / Revised: 28 March 2023 / Accepted: 7 April 2023 / Published online: 13 April 2023

Abstract

Nowadays, reports of antimicrobial resistance (AMR) against many antibiotics are increasing because of their misapplication. With this rise, there is a serious decrease in the discovery and development of new types of antibiotics amid an increase in multi-drug resistance. Unfermented *Acinetobacter baumannii* from gram-negative bacteria, which is one of the main causes of nosocomial infections and multi-drug resistance, has 4 main kinds of antibiotic resistance mechanism: inactivating antibiotics by enzymes, reduced numbers of porins and changing of their target or cellular functions due to mutations, and efflux pumps. In this study, characterization of the possible mutations in OprD (OccAB1) porins from hospital strains of *A. baumannii* were investigated using single channel electrophysiology and compared with the standard OprD isolated from wild type ATCC 19,606. For this aim, 5 *A. baumannii* bacteria samples were obtained from patients infected with *A. baumannii*, after which OprD porins were isolated from these *A. baumannii* strains. OprD porins were then inserted in an artificial lipid bilayer and the current–voltage curves were obtained using electrical recordings through a pair of Ag/AgCl electrodes. We observed that each porin has a characteristic conductance and single channel recording, which then leads to differences in channel diameter. Finally, the single channel data have been compared with the gene sequences of each porin. It was interesting to find out that each porin isolated has a unique porin diameter and decreased anion selectivity compared to the wild type.

Keywords Single-channel Electrophysiology · OprD · *A. baumannii* · Porins

✉ Fatma Doğan Güzel
fdogan@ybu.edu.tr

[1] Faculty of Engineering and Natural Sciences, Department of Biomedical Engineering, Ankara Yildirim Beyazit University, Ankara, Turkey

[2] Biotechnology Application and Research Center, Bilecik Şeyh Edebali University, Bilecik, Turkey

[3] Faculty of Science and Literature, Department of Molecular Biology and Genetics, Bilecik Seyh Edebali University, Bilecik, Turkey

[4] Cellular Therapy and Stem Cell Research Center and Translational Medicine Research and Clinical Center (ESTEM), Eskisehir Osmangazi University, Eskisehir, Turkey

[5] Faculty of Medicine, Department of Infectious Diseases and Clinical Microbiology, Adnan Menderes University, Aydin, Turkey

[6] Faculty of Medicine, Department of Infectious Diseases and Clinical Microbiology, Ankara Yildirim Beyazit University, Ankara, Turkey

[7] Department of Biotechnology and Biosafety, Eskisehir Osmangazi University, Eskisehir, Turkey

[8] Faculty of Engineering and Architecture, Department of Metallurgical and Material Engineering, Eskisehir Osmangazi University, Eskisehir, Turkey

[9] Department of Stem Cell, Institute of Health Sciences, Eskisehir Osmangazi University, Eskisehir, Turkey

[10] Translational Medicine Research and Clinical Center (TATUM), Eskisehir Osmangazi University, Eskisehir, Turkey

[11] Department of Biomedical Engineering, Eskisehir Osmangazi University, Eskisehir, Turkey

Introduction

Antimicrobial resistance is now a major global public health threat (Toner et al. 2015; Van Duin and Paterson 2016; Yadav and Kapley 2021). There are almost no new antibiotics in the advanced stages of clinical tests despite the growing number of reports about bacteria developing new resistance mechanisms against many common antibiotics of our time (Arias and Murray 2009; Bassetti et al. 2019; Fernández and Hancock 2012). In fact, our fight against bacterial infections can now be considered more challenging than human wars; there is no definitive immediate solution to possible bacterial invasion currently and in the future, and this concerns all the governments across the world (Högberg et al. 2010).

Porins are nanochannels that span the outer membrane of gram negative bacteria and allow the entry of organic and biomolecular species like nutrients, antibiotics, ions into the cell membrane (Darcan 2012; Darcan et al. 2009; Vergalli et al. 2020; Welte et al. 1995). The mechanism of multi-drug resistant (MDR) is directly related to the low permeability of antimicrobial agents through the outer membrane porins and the extrusion of the agents that are able to pass in through the outer layer by efflux pumps. It is clear that most antibiotics have to interact with porins and pass through the channel to show their full activity against the bacteria (Danelon et al. 2006; Nikaido and Pagès 2012; Poole 2001; Prajapati et al. 2021).

Therefore, as a first line of defense, bacteria can develop resistance to antibiotic agents via these outer membrane porins by modifying them, reducing their number, or changing the porins expressed for one another. In particular, infections caused by *A. baumannii* have gained considerable importance in the last few years as a result of its ability to cause a variety of nosocomial infections, including respiratory tract, bloodstream and skin, and soft-tissue infections (Abbo et al. 2005; Perez et al. 2007). *A. baumannii* is a MDR opportunistic pathogen and unquestionably a paradigm of MDR as almost all of the strains show resistance to antimicrobial agents (Costa et al. 2000; Perez et al. 2007; Vila et al. 1993).

Multi-channel and single-channel electrophysiology have been widely used to obtain insights into the mechanism of MDR over porins/substrate-specific channels and pumps (Abdali et al. 2018; Dogan Guzel et al. 2021; Guzel and Citak 2018; Lou et al. 2011; Miethke et al. 2021; Wang et al. 2020). The conductance measurement of a single channel is carried out by adding small quantities of porins (channels) to one side of an artificial bilayer forming chamber and the insertion of individual channels occurs on a time-resolvable scale (Arbing and Coulton 2003; Ebrahimi et al. 2021; Gutsmann et al. 2015; Ozturk et al. 2021). Planar lipid bilayers are almost perfect insulators, so the presence of even a single conducting channel in a lipid bilayer is readily detected (Benz et al. 1978; Gutsmann et al. 2015; Hagge et al. 2002; Montal and Mueller 1972; Mueller et al. 1962; Neher and Sakmann 1976). Signal modulations (differences in conductance) are the basis of the analysis in electrophysiology experiments. As a result of the extreme contrast in conductance levels detectable in the experiments, electrophysiology is the most suitable technique for detecting minor changes in membrane conductance, providing crucial information about the size and functional characteristics of the channel (Montal et al. 1981; Nekolla et al. 1994). In particular, substrate-specific channels of *A. baumannii* (OprD, HcaE (OccAB2), VanP (OccAB3), BenP (OccAB4), and OccAB5) have already been exclusively characterized using single-channel electrophysiology, X-ray crystallography, and molecular simulations in a previous study conducted (Zahn et al. 2016b). It was shown that the OprD possesses larger conductivity, thus a larger diameter than the others. OprD is essentially non-selective, while OccAB3 and OccAB4 display strong anion selectivity. DcaP of *A. baumannii* has later been also characterized in similar research (Bhamidimarri et al. 2018). The single-channel electrophysiology approach to characterize porins seems an important way forward for a molecular-level investigation into MDR. In terms of porins of clinical strains, Bajaj et al. reported that the single channel recording of OmpC proteins of *E. coli* isolated from a single patient over a period of treatment time proved mutations in channels (Bajaj et al. 2016).

In this study, we aimed to investigate the factors that play an important role in the resistance mechanism of *A. baumannii* using clinical samples of bacteria and to reveal the molecular mechanisms leading to new, rational, and novel drug design. In particular, the goal was to characterize the porin-mediated possible resistance mechanisms at the molecular level using OprD channels extracted from clinical samples of the bacteria by characterizing the single-channel recordings and investigating the channel diameters and selectivity values of clinical strains. To do so, OprD-type channels extracted from clinical strains of bacteria gathered from different patients were characterized at a single molecule level using high-resolution single-channel electrophysiology methodology. To the best of our knowledge, it is the first time that clinical strains of OprD-type channels of *A. baumannii* were characterized in this manner and the results were compared with sequence analysis of porins.

Materials and methods

Labelling of the channels

Ten clinical isolates and a wild-type strain were used in this study. Clinical isolates were obtained from the Medical Faculty of Adnan Menderes University. As a result of Sanger sequencing, 5 clinical isolates with different sequences were selected and the codes of the isolates are given in Table 1. A, B, C1/C2, and D were isolated from different patients, while C1 and C2 were obtained from the same patients in different time periods.

Cloning of OprD gene and isolation of OprD proteins

DNA isolation from clinical isolate and *A. baumannii* ATCC 19,606 strain were performed using the MACHEREY–NAGEL NucleoSpin Microbial DNA isolation kit. Then, the *oprD (occAB1)* gene was amplified by PCR reaction using the obtained DNAs and two primer sets; *oprD* SF1; 5′GAAATCCTAGGCCCTGAACA3′, *oprD* SR1; 5′GTGGTCCAGTTTAAACCAGG3′, *oprD* SF2; 5′CGT TGTTGGTGACGGATCAT3′ and *occAB1(oprD)*SR2; 5'GCCTAGAGTGTCGCAATTGA3') specific to OprD porin (Kaygusuz İzgördü et al. 2022). The amplified product was electrophoresed on 1% agarose and then the PCR products for Sanger sequencing were purified using MACHEREY–NAGEL NucleoSpin Gel and PCR Clean-up kit and samples were sent for sequencing. All samples submitted for sequencing were aligned using the BioEdit 7.2 sequence sequencing program. After alignment, it was determined that the oprD gene sequences of 5 clinical isolates were not identical. In strains with the *oprD* gene sequence, this gene region was amplified by PCR reaction using pLATE51 *oprD* forward (5′GGTGATGATGATGACAAGATGCTA AAAGCACAAAAACTTA3′) and pLATE51 *oprD* reverse (5′GGAGATGGGAAGTCATTAGAATAATTTCACAGG AATATCT 3′) primers and then ligated with the pLATE51 vector and transformed into *E. coli* W3110 bacteria. After transformation, recombinant *E. coli* strains were induced with 0.5 mM IPTG and then centrifuged at 12,000 rpm for 5 min at 4 °C to collect the cell pellet (approximately 1.1×10^{11} cell count). Then, proteins were purified according to the Protino denatured Ni–NTA His-tag procedure from the collected 1 g cell pellet. 5 ml of NPI-10 (50 mM NaH_2PO_4, 300 mM NaCl, 10 mM imidazole pH 8.0) buffer was added to the collected 1 g cell pellet and the pellet was dissolved in this buffer. Lysozyme was then added to this cell suspension at a final concentration of 1 mg/ml and lysed on ice for 30 min. Then, the cells were sonicated 5–6 times at 6 amplitudes. After sonication, the suspension was centrifuged at 10,000 g for 30 min at 4 °C and the supernatant was taken into a clean tube. Ni–NTA agarose, equilibrated by washing with NPI-10, was added onto the supernatant and incubated for 4 h with shaking at 9 rpm at 4 °C. After incubation, the supernatant was centrifuged at 4000 rpm for 1 min at 4 °C. After centrifugation, the supernatant was transferred to a clean tube and stored at -20 °C. 800 µl of DNPI-20 (50 mM NaH_2PO_4, 300 mM NaCl, 20 mM imidazole, 8 M urea pH 8.0) buffer was added to the pellet and the pellet was washed with this buffer. It was then centrifuged for 1 min at 4000 rpm at 4 °C. This process is repeated 3 times. After the last wash, DNPI-250 (50 mM NaH_2PO_4, 300 mM NaCl, 250 mM imidazole, 8 M urea pH 8.0) buffer was added to the pellet and centrifuged for 1 min at 4000 rpm at 4 °C. This process was repeated 3 times. Then, purified proteins were analyzed by western blot using anti-his tag antibody. Trimming was performed with TEV protease (cat. No. E027) to remove the histidine tail from the protein after checking by western blot. Then, dialysis membrane treatment was applied in 1X PBS to remove imidazole and urea from proteins and all samples were stored at − 80 °C. Porins were then diluted to 3×10^{-5} mg/ml (~0.6 nM) in a 1 wt% n-octylpolyoxyethylene detergent solution for single-channel experiments and stored at 4 °C for short-term use (Kaur et al. 2021; Ozturk et al. 2021).

Table 1 List of the names for selected clinical isolates and wild-type *strain* codes

A. baumannii source	OprD codes
Wild type	Standard
8	A
10	B
5686	C1
5687	C2
6182	D

Single channel electrophysiology

The monolayer technique of Montal and Mueller was used to form planar lipid bilayers (Gutsmann et al. 2015; Montal and Mueller 1972; Ozturk et al. 2021). In this method, planar lipid bilayer was created over an about 100 µm wide aperture opened on a Teflon film (Goodfellw, UK) with 25 µm thickness and placed in a custom-made teflon cuvette. The apertures was opened up using a custom-made controlled high voltage discharger setup (Ozturk et al. 2021). Two sides of the file form cis and trans cells of the cuvette. The teflon-made base was used to position the cuvette during the experiments. Each cell of the cuvette has the capacity to contain approximately 3 mL of electrolyte. Both sides of the surface of the teflon around the micro-pore were stained with 3 µL of a 95% hexane (Merck, DE) solution containing

1% hexadecane (Merck, DE). After the evaporation of the solvent in 15 min, a hydrophobic layer of hexadecane was formed around the micro-pore. 3 ml of 0.5 M KCl buffered with 10 mM HEPES (pH 8.0) were added to each cuvette cell, and placed in a custom-made Faraday box. Ag/AgCl electrodes (World Precision Instruments, Sarasota, FL) were immersed in each cell and attached to an amplifier (Axopatch 200B, Axon Instruments, USA) with a capacitive head-stage for electrical recordings. The electrode in the cis side was grounded, whereas the trans side electrode was connected to the head-stage. The amplifier was digitized by a digitizer (Axon Digidata 1550B, Axon Instruments, USA) and computer-controlled by Clampex 10.0 (Axon Instruments, USA). A low-pass four-pole analog Bessel filter was used for filtering data at 2–10 kHz and digitally sampled at 50–100 kHz. Clampfit 10.0 was used for data analysis. Electrical noises were reduced by grounding the Faraday cage and the amplifier. The amplifier measures the current passing through the micro-pore in pA range. First, the current crossing through the micro-pore was measured by amplifier (I_{pore} > 20 nA) to show the micro-pore is open, and then 3 µl of 5 mg/mL 1,2-diphytanoyl-sn-glycero-3-phosphocholine (DPhPC—Avanti Polar Lipids, USA) lipid solution dissolved in 1 mL 95% n-pentane (Merck, DE)) was added to both cells of the cuvette. 5 mL micro-pipettes were used for pipetting up and down the solution and the current was recorded in the amplifier until the current value decreased to 0 pA. This indicates that the planer lipid bilayer was formed around the micro-pore with a gigaohm seal. Then, single-channel experiments were performed: 1 µl of 3×10^{-5} mg/ml purified detergent-solubilized standard or clinical strains of OprD solution were added to the cis cell and different voltages (25, 50, 75, 100, 150, and 200 mV) were applied while mixing the chamber gently for channel insertion into the planer lipid bilayer membrane.

Reverse potential experiments

Selectivity experiments were performed with different electrolyte concentrations in cis and trans cells. For this, at first 1 M KCl was added to the cis and trans cells (pH: 8.0, 10 mM HEPES). Afterward, OprD channels were added into the cis cell and different voltages were applied for the insertion of the channels in the lipid bilayer. After obtaining a single channel insertion, the KCl concentration in the trans cell was diluted to 0.1 M. For dilution, approximately 20 times 1 mL of 1 M KCl solution was taken from the trans chamber, and 1 ml of 0.1 M KCl solution (pH: 8.0, 10 mM HEPES) was added instead, and the concentration in the trans side was reduced to 0.1 M. Then, the applied voltage was gradually reduced to zero. The reversal potential was calculated using a negative current at 0 voltage. The current was recorded through the amplifier and the selectivity was calculated according to the Hodgkin–Katz (GHK) equation (Arbing and Coulton 2003; Benz et al. 1985; Hille 2001; Miedema 2002):

$$\frac{P_a}{P_b} = -\frac{z_b^2\left(b_{cyt} - b_{ext}exp\left(-z_bE_{rev}F/RT\right)\right)}{z_a^2\left(a_{cyt} - a_{ext}exp\left(-z_aE_{rev}F/RT\right)\right)}x\frac{\left(1 - exp\left(-z_bE_{rev}F/RT\right)\right)}{\left(1 - exp\left(-z_aE_{rev}F/RT\right)\right)}$$

where a_{cyt}, a_{ext}, b_{cyt} and b_{ext} indicate the activities of ions with z_a and z_b valence in solution (RT/F = 25.3 mV at 20 °C) and E_{rev} is reversal potential, respectively.

Results and discussion

In this study, clinical strains of OprD from *A. baumannii* have been characterized using single channel electrophysiology and compared with the wild type to investigate the role of the channels in the development of the MDR mechanism. To do so, both single-channel recordings and microbiology results were analyzed and compared.

Clinical samples of OprD were isolated from the outer membrane of hospital strains of *A. baumannii* via a procedure previously used for the *E. coli* OmpF (Ozturk et al. 2021). DNA isolation for Sanger sequencing of OprD porin genes was first performed from clinical specimens and wild-type strain ATCC 19,606, and is shown in Fig. 1a. PCR was performed with two primers specific to the *oprD* gene with a size of approximately 700 bp from the isolated DNAs, and the obtained PCR products were purified before sequencing (Fig. 1b, c). Afterward, the samples were sent for sequencing and the *oprD* gene in the selected samples was cloned into the pLATE 51 vector and transformed into *E. coli* and the recombinant cell were confirmed using plasmid primers (Fig. 1d). OprD protein was isolated by overexpressing in the resulting recombinant cells, and the protein was confirmed by western blot analysis using anti-his antibody (Fig. 2). As a result of western blot analysis, it was determined and confirmed that the *oprD* gene was expressed and purified in *E. coli*. Gene product proteins obtained were later used in electrophysiology studies.

The gene for our target protein on the plasmid was highly expressed using a promoter induced by IPTG added. to the medium. However, these highly expressed proteins can also accumulate as insoluble aggregates known as inclusion bodies, and in this case they did. Buffers containing large amounts of denaturant (8 M urea) are used to dissolve these aggregates. The Ni–NTA purification technique used in this study enables the purification of polyhistidine-labeled proteins produced recombinantly by immobilized metal ion affinity chromatography (IMAC). Figure 2 shows that the protein was purified successfully, using Ponceau staining. In addition, with the removal of the denaturing agent after

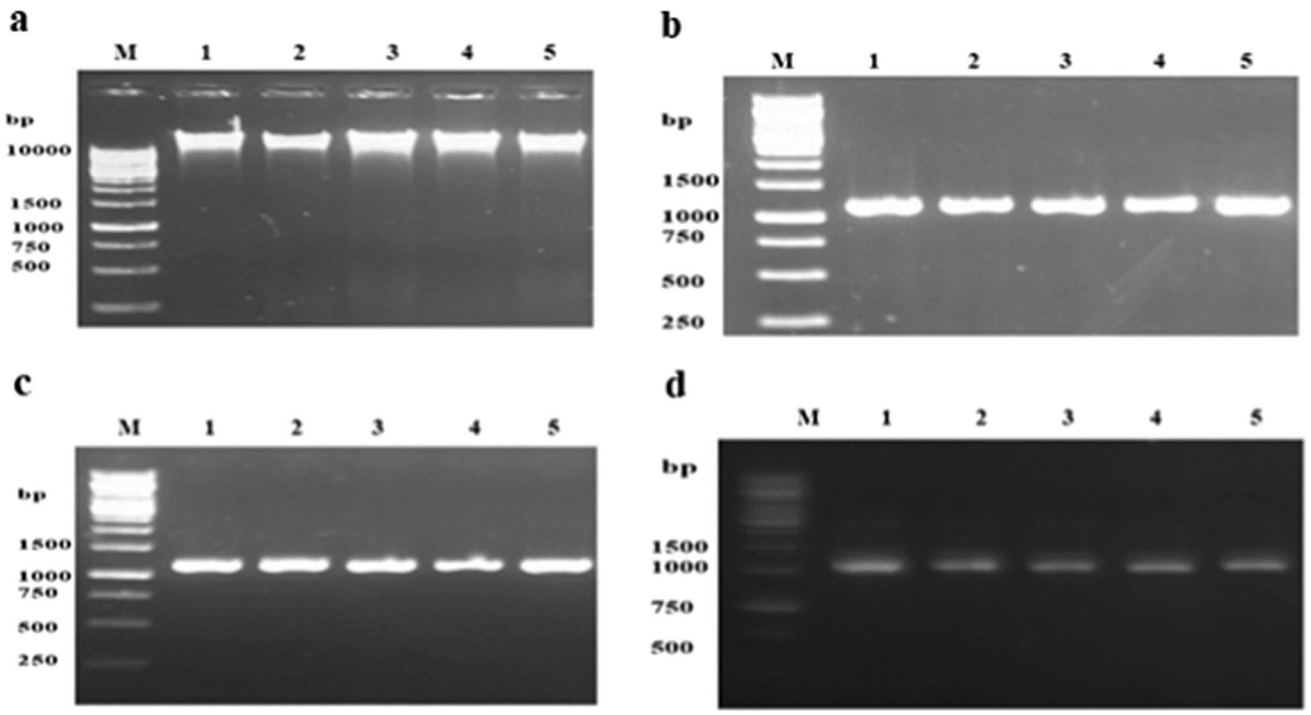

Fig. 1 **a** Genomic DNA isolation of clinical strains of *A. baumannii*, **b** purification of *A. baumannii* clinical strains *oprD* SFR1, **c** purification of *A. baumannii* clinical strains *oprD* SFR2 primer, **d** validation of the *oprD* gene with plasmid primer in recombinant *E. coli* strains [line M; Marker, line 1; strain 5686 (C1), line 2; strain 5687 (C2), line 3; strain 6182 (D), line 4; strain 8 (A), line 5; strain 10 (B)]

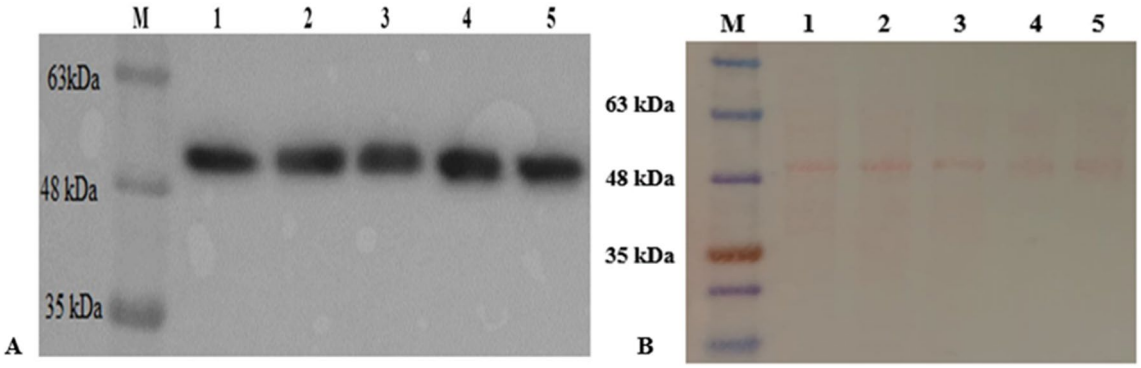

Fig. 2 **A** Western blot analysis of the expression of OprD protein in clinical *A. baumannii* strains expressed in recombinant E. coli using anti-His-tag antibodies. **B** Ponceau S staining results showing the purity of proteins prior to Western blot analysis [line M; marker, line 1; strain 5686 (C1), line 2; strain 5687 (C2), line 3; strain 6182 (D), line 4; strain 8 (**A**), line 5; strain 10 (**B**)]

the dialysis process, refolding from denatured proteins to active proteins can occur. However, there may be losses in the amount of purified protein available.

Base sequences of porin proteins of wild-type ATCC 19,606 of *A. baumannii* and OprD of 5 clinical isolates were obtained and a comparison analysis is given in Table S1. It was determined that 4 of the clinical isolates (Isolates A, C1, C2, and D) matched with wild type *A. baumannii* ATCC 19,606, and B isolate matched 100% with *A. baumannii* ATCC 17,978 when a search was made on the NCBI sequence bank. While clinical isolate D and wild type had 100% base similarity except for the X coding regions, it was determined that there was 1 amino acid difference in isolate C2 and 2 amino acid differences in strains C1 and A. Isolates C1 and C2 are strains isolated from the same patient during treatment. Therefore, a 1 amino acid difference was detected between these strains. However, a difference of 90 amino acids was detected

between the 2 wild types. Therefore, there is a 90 amino acid difference between 1 clinical isolate and the other 4 clinical isolates.

When the protein sequence data in Table S1 were further examined, we noticed that there was a change in the 47th amino acid (leucine amino acid > isoleucine) and 48th amino acid (threonine > serine) in clinical isolate C1 compared to the reference strain. Likewise, while the amino acid at position 349 was aspartic acid in the reference strain, it was converted to the amino acid glutamic acid in clinical isolate number C2.

In electrophysiology experiments, the first experiments were carried out with standard OprD. OprD has a monomer structure and has a conductance value of 535 ± 40 pS (at 50 mV, 1 M M KCl) with a channel diameter of 5–5.5 Å (Zahn et al. 2016b). The insertion of a single OprD channel in the lipid bilayer is given in Fig. 3a, and current time traces of a single OprD channel are shown in Fig. 3b.

Figure 3c shows OprD channel popping out of the bilayer upon the application of 200 mV voltage and the current returning to zero. Figure 3d shows the insertion of the second OprD channel in the lipid bilayer. It has been observed that more than one channel was usually inserted in the lipid bilayer. These standard OprD characterization experiments were repeated more than five times and all of the insertion events observed for OprD correlated with the literature. Conductance values and pore size for standard OprD were calculated using the equation:

$$r^2 = \frac{Gl}{\pi\sigma_s}$$

where G is the conductance, r is the radius of the channel, l is the length of the channel (4 nm), and σ is the conductivity of the solution (σ for 0.5 M KCl is about 5 S/m), respectively. The results show that the conductance of a single OprD channel in 0.5 M KCl solution buffered with 10 mM HEPES at pH: 7.5 in the applied voltage of 100 mV is around 235 pS. This is in agreement with the result regarding the single channel characteristic of OprD stated in the literature (Zahn et al. 2016b), and indicates that the recorded values belong to the single OprD channel. The diameter of the channel was calculated as 5 Å. This value is also compatible with the diameter (5–5.5 Å) of OprD stated in the literature (Zahn et al. 2016b). Though there are different methods for calculating the porin pore diameter like PEG partitioning, the above equation using conductance of a pore was utilized in the calculations for simplicity (Benz et al. 1985; Cruickshank et al. 1997; Guzel and Citak 2018; Harsman et al. 2012; Lakey et al. 1985; Meuser et al. 1999; Movileanu et al. 2003; Rostovtseva et al. 2002; Szabó and Zoratti 1992). The ions used for probing the pore structure have the same relative mobility while moving through the porin pore as they behave while moving in free solution. Thus, the single-channel conductances of the individual porins could be used to estimate the effective channel diameters of porins (Benz et al. 1985). It is worth mentioning that this approach only provides an approximation to the diameter calculation.

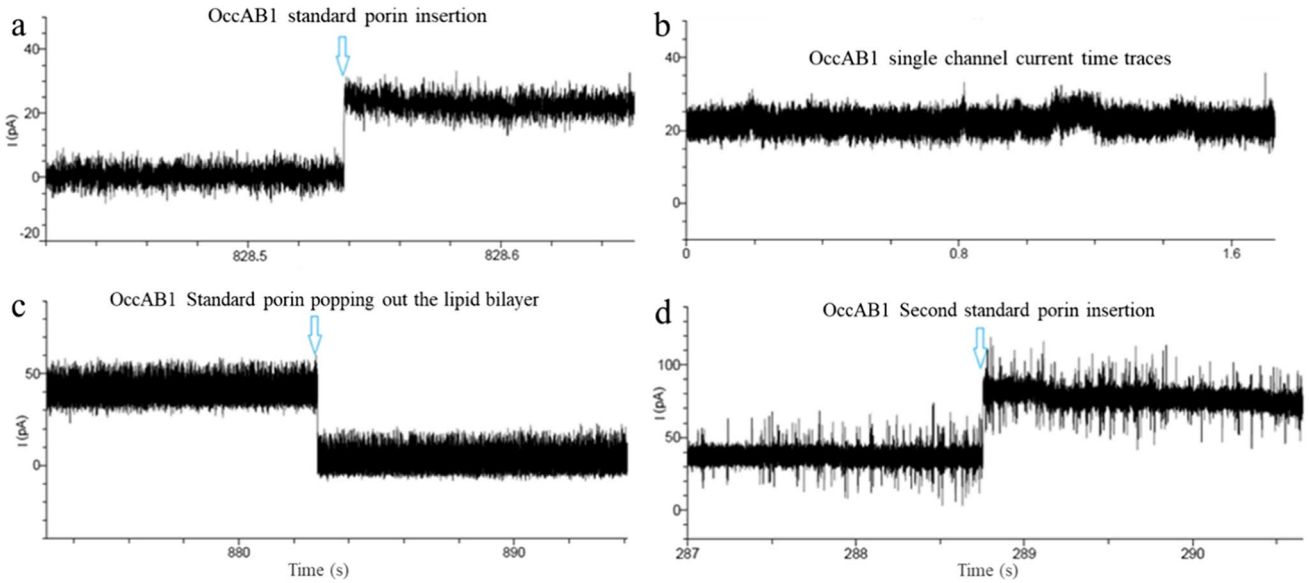

Fig. 3 Single channel recordings of standard OprD channel. **a** Insertion of single OprD channel in the lipid bilayer, **b** current time traces for single OprD channel, **c** popping out of the OprD channel from the lipid bilayer at 200 mV applied voltage, **d** insertion of the second OprD channel at 200 mV applied voltage. Data were recorded at 100 mV, in 0.5 M M KCl, HEPES buffer 10 mM (pH = 7.5), sampled at a frequency of 100 kHz, and filtered at 5 kHz)

Unlike solid-state nanopores, protein pores require more detailed study. As mentioned next, the channel insertion of the clinical samples was not as easy as the insertion of other classical porins, making difficult experiments for any detailed study on pore diameter calculations.

The success rate of insertion of clinical samples of OprD into the lipid bilayer was comparatively low as opposed to the insertion of OmpF and wild-type OprD (some of the recorded insertions are shown in Figs. S1–S3). It is well-known that OmpF inserts into the lipid bilayer easily; however, we found that wild-type OprD insertion into the lipid bilayer was relatively difficult. Insertion of OprD clinical samples was even more difficult for some reason, which cannot be explained at this point but which may relate to bioactivity or stability after expression. Among the clinical samples, insertion of the C1 and C2 channels in the planer lipid bilayer were more difficult in comparison with the others. During the experiments, we have only 4 successful insertions for C2, while the number of successful insertions for C1 was more than 20 times. Figure 4 shows the current–time traces for single channel recordings of OprD channels and Table 2 shows the channel diameter for each one. While the calculated channel diameter for standard OprD was found to be 5.0 ± 0.11 Å and close to OprD diameter literature value (5–5.5 Å) (Zahn et al. 2016b), different channel diameters were obtained for clinical samples ($A \cong 4.4$ Å ± 0.09, $B \cong 4.8$ Å ± 0.09, $C1 \cong 4.4$ Å ± 0.12, $C2 \cong 4.3 \pm 0.04$ Å and $D \cong 4.6 \pm 0.05$ Å). C2 has the smallest channel diameter, while B is the widest in terms of the channel size. These results show decreases in channel diameter in all clinical strains of OprD. Decrease in channel diameter is one of the defense and resistance mechanisms of bacteria against antibiotics (Cox and Wright 2013; Decad and Nikaido 1976; Fernández and Hancock 2012). This is a sign of the impact of mutations in the clinical samples in general and in particular the constriction zone of OprD from clinical strains is narrower compared with that of the wild-type one. The results may also indicate that these decreases in channel diameter could be part of an *A. baumannii* resistance mechanism, on the assumption that the OprD isolated from clinical strains is directly involved. Another significant finding is the identical differences in the recorded current–time traces among all 6 OprD channels. This is also probably a consequence of mutation in clinical strains in comparison with standard OprD (Fig. 4).

B and D strains show fluctuations in their current–time trace, whereas A, and C1 are more stable. C2 has the most stable current–time trace with the least fluctuations. There is some noise in some of the recordings such as that of C2, this may be a result of electrical interference from the outside (noise caused by power sources, light, electrical connections etc.). Insertion of C2 into the lipid bilayer was relatively difficult; therefore, repetitive experiments could not be performed to obtain signals without noise.

Last, we conducted selectivity experiments to understand if mutations also change the anion/cation selectivity of the channels which is a definitive parameter for the uptake of charged molecules and antibiotics. In most of the OprD channels, the distribution of charged parts is asymmetric. So that the extracellular side of the channel may exclude/collect in a different way than the cytosol or the intermembrane side of the channel (Aguilella et al. 2011; Hille 2001). This asymmetric character can be analyzed by selectivity measurements in which measured zero-current potentials (mV) vary depending on the channel nature and could be used as an indicative sign of selectivity. For an anion-selective channel, negative values for mV are observed and vice versa.

Table 2 shows the ion selectivity results for OprD channels calculated by the results of reverse potential experiments. Selectivity results also show differences among the OprD channels. While the OprD channels were described as non-ion selective in literature (Zahn et al. 2016b), our results show that clinical OprD channels are anion-selective. Although all of the OprD channels show anion selectivity, the high anion selectivity was observed for standard OprD (P_{K^+}/P_{Cl^-}: 0.030). A decrease in anion selectivity detected for clinical samples (calculated P_{K^+}/P_{Cl^-} for channels: A: 0.611, B: 0.416, C1: 0.730, C2: 0.709, D: 0.809) in general. There was a little difference in selectivity values between C1 and C2 that was isolated from the same patient at different periods of time. When looking into the sequencing results, it was found that the DNA sequence for D is the same as the wild type, except the regions encoded with X (Fig. 5 and Table S1). In Sanger sequencing, read quality is often not homogeneous along the read length. The beginning and end regions generally have lower read quality than other regions. In the Sanger data obtained in the study, due to the quality of the reads corresponding to amino acid 27 of *A. baumannii* ATCC 19,606 and amino acids 378, 421, 423, 429, and 432 of sample D, these regions were coded with X, which may indicate any amino acid. The sequences of the codons corresponding to these amino acids and the amino acids encoded by these codons are given in Table S2. The region of each amino acid was sequenced twice and each time only one of the reads was found to be identical to the reference *A. baumannii* NCBI ATCC 19,606 genome. This suggests that there may be some differences in the sequencing of the sample D and the wild type. In our study, sequencing accuracy could have been improved by sequencing the same region multiple times using different sequencing methods. However, since the cost of sequencing is low and the gene region to be sequenced is small, the gold standard Sanger method was chosen for sequencing.

Single-channel traces look similar in characteristics except for that the noise and the conductance values of the

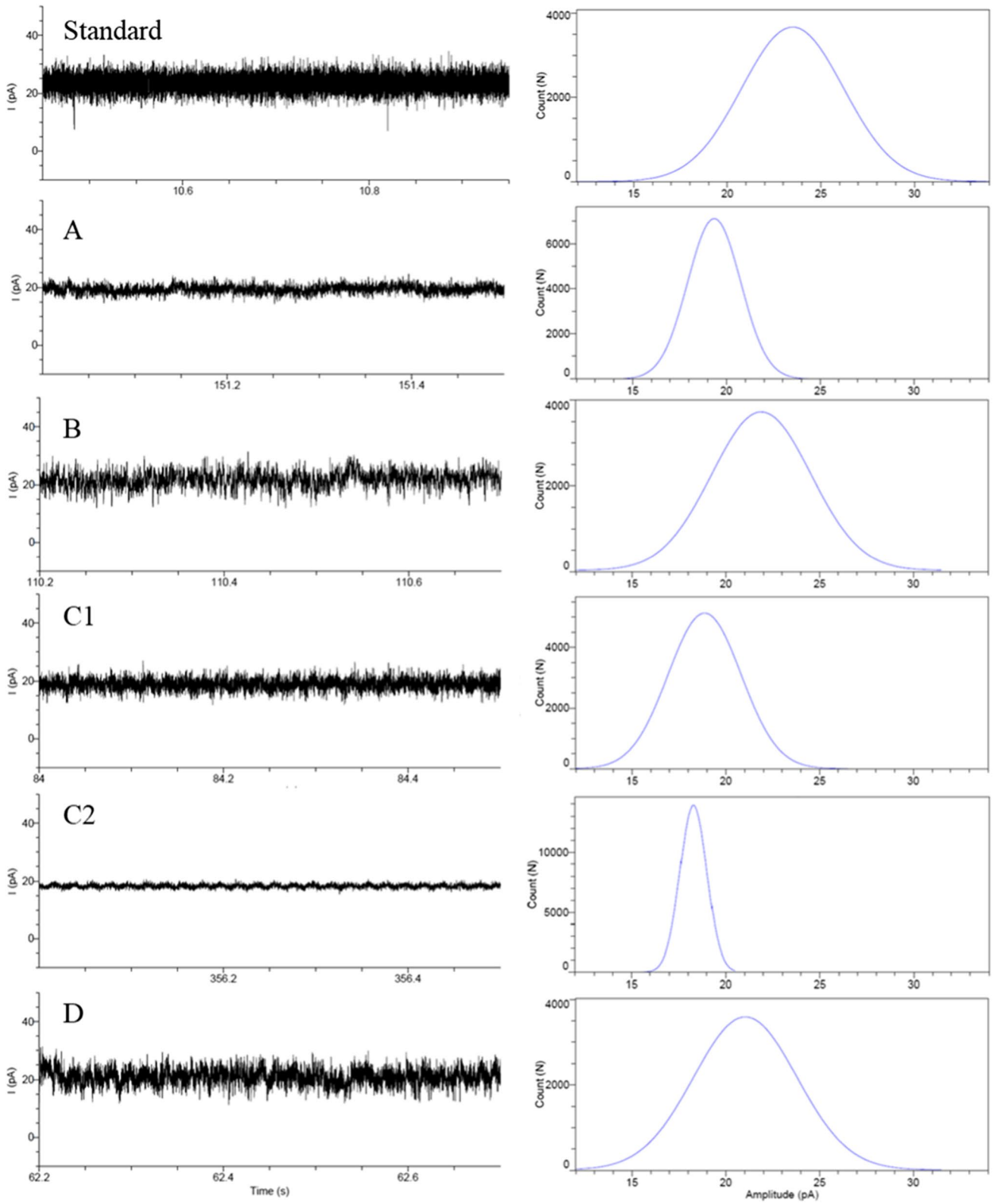

Fig. 4 Single channel current time traces and histograms of standard and clinical samples of OprD (Standard, **A**, **B**, **C1**, **C2**, and **D**, respectively). Standard channel: (100 mV, 0.5 M M KCl, HEPES buffer 10 mM, pH = 7.5, sampling frequency 100 kHz, filtering at 5 kHz). Clinical samples: (100 mV, 0.5 M M KCl, HEPES buffer 10 mM, pH = 8, sampling frequency 50 kHz, filtering at 2 kHz)

Table 2 Conductance (100 mV, 0.5 M M KCl, HEPES buffer 10 mM, pH = 7.5), calculated diameter and selectivity values for standard and clinical OprD (A, B, C1, C2, and D) channels

OprD	Conductance at 100 mV (pS)	Diameter Å	Selectivity (P_{K^+}/P_{Cl^-})
Standard	235	5.0 ± 0.11	0.030
A	193	4.4 ± 0.09	0.611
B	219	4.8 ± 0.09	0.416
C1	189	4.4 ± 0.12	0.730
C2	183	4.3 ± 0.04	0.709
D	210	4.6 ± 0.05	0.809

wild type and sample D are closer compared with other clinical samples, it is interesting to find that the selectivity values (0.030 and 0.805, respectively) are very different. As mentioned above, the wild type and D porin have high similarity in sequences, but the selectivity of standard and D porin are very different, almost 20 fold, although being expressed in similar conditions, while selectivity of D protein is in line with previously published data (Zahn et al. 2016b). According to the standard OprD sequence, there are 2 amino acid differences in the A and C1 sequences and 1 amino acid difference in the C2 sequence. These are amino acids 47 and 48, and amino acid 346, respectively, and are located in the β-strand. The sequence of clinical sample B differs by 90 amino acids from the standard OprD. There is also a deletion of 10 amino acids. The OprD has 18 β-strands, and β-strands have the main influence on the permeability data of the channel as a constriction zone. L3 and L7 loops are responsible for the constriction zone, which mostly governs selectivity and permeability. It is the β-strand that affects the diameter and conductivity of the pore. When DNA sequence results are evaluated, no mutations are seen in these loops except for sample B, in which there are mutations in the β-strand and deletion was seen in loops L7 and L11. Sample B has the closest value to the wild-type conductance and thus diameter, even though it is the only clinical isolate that possesses a deletion in its β-strand. As opposed to that, the selectivity value is the closest to that of the standard OprD. Conductance values for samples A, C1, and C2 are relatively different than that of the standard OprD. Among samples C1 and C2, there is a slight difference in both conductance and selectivity. Mutations and deletions in the 3D structure of the OprD protein are shown in Fig. 6.

When the conductance and channel diameter results obtained from the single channel electrophysiology experiments are evaluated together with the results of the sequence analysis, it becomes clear that the single-channel current time traces obtained for each OprD channel is different with identical characteristics in signal fluctuations, conductance level, diameter and selectivity, this is one of the most important results from the experiments. The difference in the current time traces shows that the current modulations that arise from the movements of the loops are also different. Interestingly, the diameter values were calculated to be low in all clinical strains with point mutations. Even though sample D has the same sequence with the standard one, it also shows differences in respective values. The selectivity of standard and D porin are very different, almost 20 folds. Compared to the work carried out by Zhan et al. (2016b), it is clear that there are differences in various findings. While selectivity of wild-type porin is different from literature, D protein selectivity is in line with the study conducted by Zahn et al. This may be due to the differences in expression approaches: we sequenced the oprD gene region of *A. baumannii* ATCC 19,606. This sequence has been compared to both AB307-0294 and ATCC 19,606 found in NCBI. As a result of the comparison, it was determined that all 3 sequences were 100% identical except the regions encoded with X. Due to the reading quality of the Sanger method, as also stated above, there is a possibility of mutations in some regions in the sequence of sample D. Possibility of a point mutation may results in high change in electrophysiology experiments, as previously shown by Lou et al. (2011). In addition, protein gene expression was performed in different plasmids, while the transformation was also performed in different strains of *E. Coli*. These differences may slightly change the folding shape that provides the 3D structure of the proteins and may differentiate the measurement results. Changes in 3D structure may include variation in lengths, conformation and orientation of extracellular loops, and charge distribution around the loops and at the constriction zone. Confirmation for the reasons leading to the changes requires further studies with X-ray crystallography.

D. Güzel et al. recently reported that porins show different characteristics when homologous expression of the native protein was used, where any issues with membrane structure, coding and aggregation is overcome (Dogan Guzel et al. 2021). In the environments of intensive care units in the clinic, microorganisms are exposed to different chemicals and disinfectants, thereby different environments than their laboratory environment, such as pH. Ghai et al. showed that pH, temperature, oxidative stress, and toxic compounds change the expression level of OmpC and OmpF (Ghai and Ghai 2017). Its direct effect on porins (3D folding of the protein, its location into the lipid cell membrane, etc.) is not fully known. The differences in clinical samples should perhaps be more discussed in the context of their exposure to the chemical changes in their surroundings. It seems that it is hard to exclusively explain the reason behind the changes in light of only sequencing results. As mentioned in above, the ion selectivity of Porin D changes already by a factor of 20 as compared to standard. This is clear that, small change of the diameter of the channel cannot result in such a large change of selectivity. This must be the result of a change in

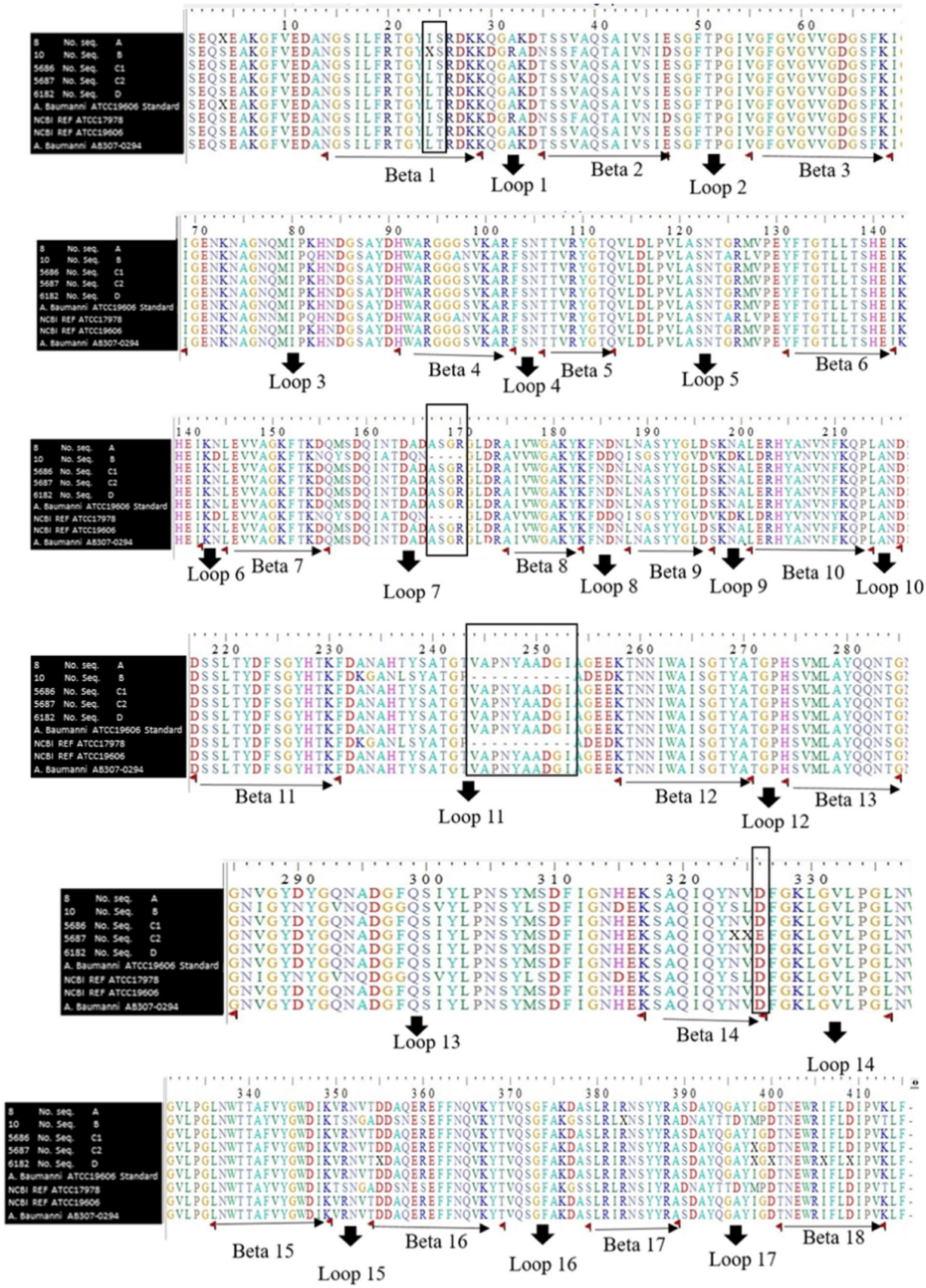

Fig. 5 ESPript sequence alignment of OprD channels (wild type and clinical samples) of *A. baumannii*

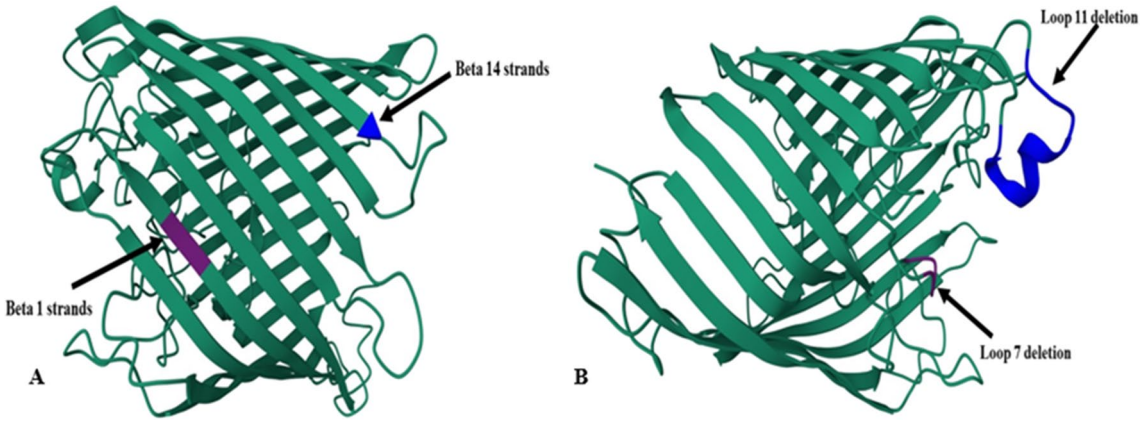

Fig. 6 **A** Mutations of A, C1 and C2 isolates relative to *A. baumannii* ATCC 19,606 wild type, **B** deletions observed in B according to wild-type *A. baumannii* ATCC 19,606 and in wild-type *A. baumannii* ATCC 17978*A*. Represented by permission from Protein Data Bank web page (Zahn et al. 2016a) (https://www.rcsb.org/3d-view/5DL5)

3-D structure and/or a mutation of an amino acid. The primary structures of OprD channels shown in Fig. 5, indicate that mutations are not directly responsible for the change in selectivity. Probably change in 3-D structure of channels can result in this high change in anion selectivity. Performing Molecular Dynamics (MD) simulations in further stages may help clarify the complexity, while X-ray analysis may also be useful.

Conclusion

In this study, OprD porins were isolated from wild-type *A. baumannii* and 5 different *A. baumannii* clinical strains. Single channel electrophysiology current–time traces were obtained for OprD channels. Conductance and channel diameter were calculated for all samples. Different conductance and diameter values were obtained for every 6 samples and as a result, it was determined that there were differences in OprD channels from clinical strains in comparison with standard OprD. It is unexpectedly striking to see that the single-channel recordings and associated results are different between clinical samples and standard OprD and this is almost independent from the mutations. We believe that our results would help to understand that the clinical samples produce different single-channel characteristics.

Supplementary Information The online version contains supplementary material available at https://doi.org/10.1007/s00249-023-01651-2.

Acknowledgements The authors would like to acknowledge funding from TUBITAK under grant number 117S114. The authors would also like to thank Prof. İ. Agah İnce, Dr. Araz N. Dizaji, Prof. Mathias Winterhalter and Dr. Daniel Pletzer for useful discussions in general and Prof. Barış Otlu for useful discussions during the selection of clinical samples.

Data availability All data generated or analysed during this study are included in this published article.

Declarations

Conflict of interest The authors declare that they have no conflict of interest.

References

Abbo A, Navon-Venezia S, Hammer-Muntz O, Krichali T, Siegman-Igra Y, Carmeli Y (2005) Multidrug-resistant *Acinetobacter baumannii*. Emerg Infect Dis 11:22. https://doi.org/10.3201/eid1101.040001

Abdali N, Younas F, Mafakheri S, Pothula KR, Kleinekathöfer U, Tauch A, Benz R (2018) Identification and characterization of smallest pore-forming protein in the cell wall of pathogenic *Corynebacterium urealyticum* DSM 7109. BMC Biochem 19:1–18. https://doi.org/10.1186/s12858-018-0093-9

Aguilella VM, Queralt-Martín M, Aguilella-Arzo M, Alcaraz A (2011) Insights on the permeability of wide protein channels: measurement and interpretation of ion selectivity. Integr Biol 3:159–172. https://doi.org/10.1039/c0ib00048e

Arbing M, Coulton J (2003) Planar lipid bilayer analyses of bacterial porins; the role of structure in defining function Membrane Science and technology, vol 7. Elsevier, Amsterdam, pp 371–390. https://doi.org/10.1056/NEJMp0804651

Arias CA, Murray BE (2009) Antibiotic-resistant bugs in the 21st century—a clinical super-challenge. N Engl J Med 360:439–443. https://doi.org/10.1056/NEJMp0804651

Bajaj H, Scorciapino MA, Moynié L, Page MG, Naismith JH, Ceccarelli M, Winterhalter M (2016) Molecular basis of filtering carbapenems by porins from β-lactam-resistant clinical strains of *Escherichia coli*. J Biol Chem 291:2837–2847. https://doi.org/10.1074/jbc.M115.690156

Bassetti M, Giacobbe DR, Peghin M, Irani P (2019) A look at clinical trial design for new antimicrobials for the adult population. Expert Rev Clin Pharmacol 12:1037–1046. https://doi.org/10.1080/17512433.2019.1680283

Benz R, Janko K, Boos W, Läuger P (1978) Formation of large, ion-permeable membrane channels by the matrix protein (porin) of

Escherichia coli. Biochimica Et Biophysica Acta (BBA)-Biomembranes 511:305–319. https://doi.org/10.1016/0005-2736(78)90269-9

Benz R, Schmid A, Hancock R (1985) Ion selectivity of gram-negative bacterial porins. J Bacteriol 162:722–727. https://doi.org/10.1128/jb.162.2.722-727.1985

Bhamidimarri SP, Zahn M, Prajapati JD, Schleberger C, Söderholm S, Hoover J, West J, Kleinekathöfer U, Bumann D, Winterhalter M (2018) A multidisciplinary approach towards identification of novel antibiotic scaffolds for *Acinetobacter baumannii*. bioRxiv. https://doi.org/10.1101/306035

Costa S, Woodcock J, Gill M, Wise R, Barone A, Caiaffa H, Levin A (2000) Outer-membrane proteins pattern and detection of β-lactamases in clinical isolates of imipenem-resistant *Acinetobacter baumannii* from Brazil. Int J Antimicrob Agents 13:175–182. https://doi.org/10.1016/S0924-8579(99)00123-5

Cox G, Wright GD (2013) Intrinsic antibiotic resistance: mechanisms, origins, challenges and solutions. Int J Med Microbiol 303:287–292. https://doi.org/10.1016/j.ijmm.2013.02.009

Cruickshank CC, Minchin RF, Le Dain A, Martinac B (1997) Estimation of the pore size of the large-conductance mechanosensitive ion channel of *Escherichia coli*. Biophys J 73:1925–1931. https://doi.org/10.1016/S0006-3495(97)78223-7

Danelon C, Nestorovich EM, Winterhalter M, Ceccarelli M, Bezrukov SM (2006) Interaction of zwitterionic penicillins with the OmpF channel facilitates their translocation. Biophys J 90:1617–1627. https://doi.org/10.1529/biophysj.105.075192

Darcan C (2012) Expression of OmpC and OmpF porin proteins and survival of *Escherichia coli* under photooxidative stress in Black Sea water. Aquat Biol 17:97–105. https://doi.org/10.3354/ab00458

Darcan C, Özkanca R, İdil Ö (2009) The role of RpoS, H-NS and AcP on the pH-dependent OmpC and OmpF porin expressions of *Escherichia coli* at different pH. Afr J Biotechnol. https://doi.org/10.5897/AJB

Decad GM, Nikaido H (1976) Outer membrane of gram-negative bacteria. XII. Molecular-sieving function of cell wall. J Bacteriol 128:325–336. https://doi.org/10.1128/jb.128.1.325-336.1976

Dogan Guzel F, Pletzer D, Norouz Dizaji A, Al-Nahas K, Bajrai M, Winterhalter M (2021) Towards understanding single-channel characteristics of OccK8 purified from *Pseudomonas aeruginosa*. Eur Biophys J 50:87–98. https://doi.org/10.1007/s00249-021-01498-5

Ebrahimi A, Ergun T, Kaygusuz O, Darcan C, Avci H, Noruz-Dizaji A, Ozturk SB, Rahmet Guner H, Dogan Guzel F (2021) Characterization of Porins from Hospital Strains of Acinetobacter Baumannii by Single Channel Electrophysiology 4th International Eurasian Conference on Biological and Chemical Sciences (EurasianBioChem 2021) Ankara, Turkey, pp 42–43

Fernández L, Hancock RE (2012) Adaptive and mutational resistance: role of porins and efflux pumps in drug resistance. Clin Microbiol Rev 25:661–681. https://doi.org/10.1128/CMR.00043-12

Ghai I, Ghai S (2017) Exploring bacterial outer membrane barrier to combat bad bugs. Infect Drug Resistance 10:261. https://doi.org/10.2147/IDR.S144299

Gutsmann T, Heimburg T, Keyser U, Mahendran KR, Winterhalter M (2015) Protein reconstitution into freestanding planar lipid membranes for electrophysiological characterization. Nat Protoc 10:188–198. https://doi.org/10.1038/nprot.2015.003

Guzel FD, Citak F (2018) Development of an on-chip antibiotic permeability assay with single molecule detection capability. IEEE Trans Nanobiosci 17:155–160. https://doi.org/10.1109/TNB.2018.2809592

Hagge SO, De Cock H, Gutsmann T, Beckers F, Seydel U, Wiese A (2002) Pore formation and function of phosphoporin PhoE of *Escherichia coli* are determined by the core sugar moiety of lipopolysaccharide. J Biol Chem 277:34247–34253. https://doi.org/10.1074/jbc.M201950200

Harsman A, Niemann M, Pusnik M, Schmidt O, Burmann BM, Hiller S, Meisinger C, Schneider A, Wagner R (2012) Bacterial origin of a mitochondrial outer membrane protein translocase: new perspectives from comparative single channel electrophysiology*◆. J Biol Chem 287:31437–31445

Hille B (2001) Ion channels of excitable membranes. Sinauer Associates Inc., Sunderland, p 814

Högberg LD, Heddini A, Cars O (2010) The global need for effective antibiotics: challenges and recent advances. Trends Pharmacol Sci 31:509–515. https://doi.org/10.1016/j.tips.2010.08.002

Kaur J, Ghorbanpoor H, Öztürk Y, Kaygusuz Ö, Avcı H, Darcan C, Trabzon L, Güzel FD (2021) On-chip label-free impedance-based detection of antibiotic permeation. IET Nanobiotechnol 15:100–106. https://doi.org/10.1049/nbt2.12019

Kaygusuz İzgördü Ö, Darcan C, Doğan Güzel F (2022) Cloning, Expression, and Purification of A. baumannii OccAB1 Porin Protein in *Escherichia coli*. Osmaniye Korkut Ata University Journal of The Institute of Science and Technology xxxxx:xxxxx (Under Review)

Lakey J, Watts J, Lea E (1985) Characterisation of channels induced in planar bilayer membranes by detergent solubilised Escherichia coli porins. Biochimica Et Biophysica Acta (BBA)-Biomembranes 817:208–216. https://doi.org/10.1016/0005-2736(85)90022-7

Lou H, Chen M, Black SS, Bushell SR, Ceccarelli M, Mach T, Beis K, Low AS, Bamford VA, Booth IR (2011) Altered antibiotic transport in OmpC mutants isolated from a series of clinical strains of multi-drug resistant *E. coli*. PloS One 6:e25825. https://doi.org/10.1371/journal.pone.0025825

Meuser D, Splitt H, Wagner R, Schrempf H (1999) Exploring the open pore of the potassium channel from *Streptomyces lividans*. FEBS Lett 462:447–452. https://doi.org/10.1016/s0014-5793(99)01579-3

Miedema H (2002) Surface potentials and the calculated selectivity of ion channels. Biophys J 82:156–159. https://doi.org/10.1016/S0006-3495(02)75382-4

Miethke M, Pieroni M, Weber T, Brönstrup M, Hammann P, Halby L, Arimondo PB, Glaser P, Aigle B, Bode HB (2021) Towards the sustainable discovery and development of new antibiotics. Nat Rev Chem 5:726–749. https://doi.org/10.1038/s41570-021-00313-1

Montal M, Mueller P (1972) Formation of bimolecular membranes from lipid monolayers and a study of their electrical properties. Proc Natl Acad Sci 69:3561–3566. https://doi.org/10.1073/pnas.69.12.3561

Montal M, Darszon A, Schindler H (1981) Functional reassembly of membrane proteins in planar lipid bilayers. Q Rev Biophys 14:1–79. https://doi.org/10.1017/s0033583500002079

Movileanu L, Cheley S, Bayley H (2003) Partitioning of individual flexible polymers into a nanoscopic protein pore. Biophys J 85:897–910. https://doi.org/10.1016/s0006-3495(03)74529-9

Mueller P, Rudin DO, Ti Tien H, Wescott WC (1962) Reconstitution of cell membrane structure in vitro and its transformation into an excitable system. Nature 194:979–980. https://doi.org/10.1038/194979a0

Neher E, Sakmann B (1976) Single-channel currents recorded from membrane of denervated frog muscle fibres. Nature 260:799–802. https://doi.org/10.1038/260799a0

Nekolla S, Andersen C, Benz R (1994) Noise analysis of ion current through the open and the sugar-induced closed state of the LamB channel of *Escherichia coli* outer membrane: evaluation of the sugar binding kinetics to the channel interior. Biophys J 66:1388–1397. https://doi.org/10.1016/S0006-3495(94)80929-4

Nikaido H, Pagès J-M (2012) Broad-specificity efflux pumps and their role in multidrug resistance of Gram-negative bacteria. FEMS Microbiol Rev 36:340–363. https://doi.org/10.1111/j.1574-6976.2011.00290.x

Ozturk Y, Ebrahimi A, Dizaji AN, Kaygusuz O, Bafna JA, Winterhalter M, Cankaya G, Darcan C, Guzel FD (2021) Rapid fabrication of teflon apertures by controlled high voltage pulses for formation of free standing planar lipid bilayer membrane. Biomed Microdevice 23:1–9. https://doi.org/10.1007/s10544-021-00553-4

Perez F, Hujer AM, Hujer KM, Decker BK, Rather PN, Bonomo RA (2007) Global challenge of multidrug-resistant *Acinetobacter baumannii*. Antimicrob Agents Chemother 51:3471–3484. https://doi.org/10.1128/AAC.01464-06

Poole K (2001) Multidrug resistance in Gram-negative bacteria. Curr Opin Microbiol 4:500–508. https://doi.org/10.1016/s1369-5274(00)00242-3

Prajapati JD, Kleinekathöfer U, Winterhalter M (2021) How to enter a bacterium: bacterial porins and the permeation of antibiotics. Chem Rev 121:5158–5192. https://doi.org/10.1021/acs.chemrev.0c01213

Rostovtseva TK, Nestorovich EM, Bezrukov SM (2002) Partitioning of differently sized poly (ethylene glycol) s into OmpF porin. Biophys J 82:160–169. https://doi.org/10.1016/S0006-3495(02)75383-6

Szabó I, Zoratti M (1992) The mitochondrial megachannel is the permeability transition pore. J Bioenerg Biomembr 24:111–117. https://doi.org/10.1007/BF00769537

Toner E, Adalja A, Gronvall GK, Cicero A, Inglesby TV (2015) Antimicrobial resistance is a global health emergency. Health Security 13:153–155. https://doi.org/10.1089/hs.2014.0088

Van Duin D, Paterson DL (2016) Multidrug-resistant bacteria in the community: trends and lessons learned. Infect Dis Clin 30:377–390. https://doi.org/10.1016/j.idc.2016.02.004

Vergalli J, Bodrenko IV, Masi M, Moynie L, Acosta-Gutierrez S, Naismith JH, Davin-Regli A, Ceccarelli M, Van den Berg B, Winterhalter M (2020) Porins and small-molecule translocation across the outer membrane of Gram-negative bacteria. Nat Rev Microbiol 18:164–176. https://doi.org/10.1038/s41579-019-0294-2

Vila J, Marcos A, Marco F, Abdalla S, Vergara Y, Reig R, Gomez-Lus R, Jimenez de Anta T (1993) In vitro antimicrobial production of beta-lactamases, aminoglycoside-modifying enzymes, and chloramphenicol acetyltransferase by and susceptibility of clinical isolates of *Acinetobacter baumannii*. Antimicrob Agents Chemother 37:138–141. https://doi.org/10.1128/AAC.37.1.138

Wang J, Terrasse R, Bafna JA, Benier L, Winterhalter M (2020) Electrophysiological characterization of transport across outer-membrane channels from gram-negative bacteria in presence of lipopolysaccharides. Angew Chem Int Ed 59:8517–8521. https://doi.org/10.1002/anie.201913618

Welte W, Nestel U, Wacker T, Diederichs K (1995) Structure and function of the porin channel. Kidney Int 48:930–940. https://doi.org/10.1038/ki.1995.374

Yadav S, Kapley A (2021) Antibiotic resistance: global health crisis and metagenomics. Biotechnology Rep 29:e00604. https://doi.org/10.1016/j.btre.2021.e00604

Zahn M, Basle A, van den Berg B (2016a) Crystal structure of Acinetobacter baumannii OccAB1. Protein Data Bank https://www.rcsb.org/3d-view/5DL5. doi:https://doi.org/10.2210/pdb5DL5/pdb

Zahn M, Bhamidimarri SP, Baslé A, Winterhalter M, Van den Berg B (2016b) Structural insights into outer membrane permeability of *Acinetobacter baumannii*. Structure 24:221–231. https://doi.org/10.1016/j.str.2015.12.009